

The Frequency Dependence of Quantized Current Plateaus Induced by Surface Acoustic Waves Through a Quantum Point Contact

Minky SEO, Hana KIM and Yunchul CHUNG*

Department of Physics, Pusan National University, Busan 609-735

Nam KIM,[†] Byung-Chill WOO and Jinhee KIM

Korea Research Institute of Standard and Science, Daejeon 306-600

(Received 17 September 2009, in final form 20 October 2009)

The acousto-electric current through a split gate induced by surface acoustic waves (SAW) was studied. The current plateaus were observed when proper frequencies of SAW were applied to the device. The resulting current plateau values corresponded to nef , where n is the number of electrons transferred per cycle and f is the induced SAW frequency. Also, the width of the plateaus was found to change periodically as the SAW frequency changed. Unwanted coupling of the RF signal (applied to inter-digitized transducer to produce SAW) to the gate of QPC were found to cause the changes in plateaus width.

PACS numbers: 72.50.+b, 72.70.+m, 72.90.+y

Keywords: Current standard, Surface acoustic wave, Quantum dot, Quantum point contact

DOI: 10.3938/jkps.55.2482

I. INTRODUCTION

There have been numerous efforts to realize a quantum current standard since the classical current standard defined by the Biot-Savart law does not offer sufficient accuracy to meet modern developments in electronics. The basic idea of the quantum current standard is to transport integer multiples of electrons per cycle by modulating the potential barriers of a single electron transistor periodically with a frequency of f . This method will give currents of $I = nef$, where n is the number of electrons transferred at a time and f is the modulation frequency. One of the pioneering works was done with a quantum dot by modulating the gates of a quantum dot [1–3] in turnstile fashion [4]. Also a similar work was done with a metallic single electron transistor [5]. These works showed the possibility of a new current standard by demonstrating that a quantized current could indeed be achieved in a controllable way. However, the currents achieved with the methods mentioned above were rather low because the relatively long RC time constant of the circuit limited the operating frequency. The resulting operating frequencies were to be around a few tens of MHz, and this resulted in a few pA output current, which limited the application as a current standard. Recently, there were reports that the operating frequency

could be increased up to a few hundreds of MHz [6–8]. To overcome such problem, a surface-acoustic-wave (SAW)-driven electron pump [9–11] was adopted. The SAW-driven pump can produce a relatively large current by delivering GHz range surface acoustic waves through a quasi 1-D conduction channel. Conventionally, a 1-D conduction channel is fabricated using a 2-D electron gas system based on AlGaAs-GaAs hetero-junction [9–11]. Recently, there have been new attempts to use carbon-nanotubes as 1-D conduction channel [12,13].

In this work, we have studied SAW-induced acousto-electric currents through a split gate. The SAW generated by a interdigitated transducer (IDT) were delivered through a metallic split gate, which served as a quantum point contact (QPC). As the SAW moves along a QPC, the SAW modulates the conduction band energy profile to a sinusoidal shape in the direction of the SAW propagation. The superposition of the SAW-induced potential and the conduction band profile of the QPC forms a moving quantum dot. Since the number of electrons inside the quantum dot is quantized by integer numbers, this scheme allows one to transfer an integer number of electrons per single SAW cycle. Hence, the transferred currents becomes $I = nef$, where f is the frequency of the SAW and n is the number of electrons inside the moving quantum dot. Since the SAW can be generated up to a few GHz by applying an rf signal to an IDT, considerably large currents can be generated compared to the turnstile-type device. However, since a high-frequency

*E-mail: ycchung@pusan.ac.kr; Fax: +82-51-513-7664

[†]E-mail: namkim@kriss.re.kr; Fax: +82-42-863-5953

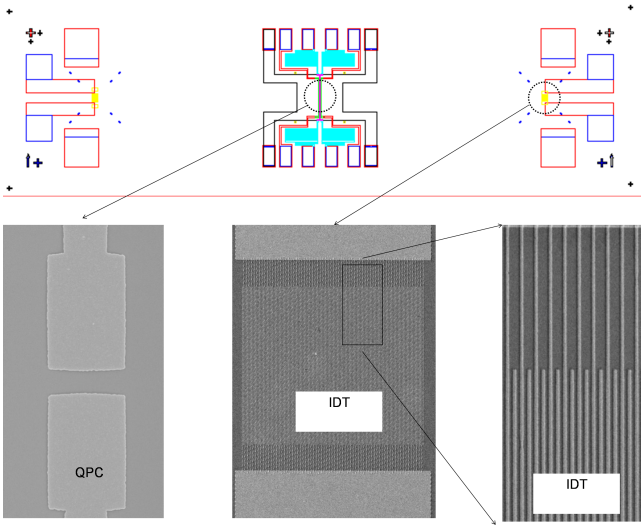


Fig. 1. The upper figure is the design of the device. The SEM pictures of the IDT and the QPC are shown in the lower part of the figure. The width of the QPC is about $2\ \mu\text{m}$ and the gap between the two metallic gates is about $800\ \text{nm}$. The IDT consists of 70 pairs of electrodes, and the overlap of the electrodes is $70\ \mu\text{m}$.

rf signal can be easily picked up by a QPC due to the stray capacitance between the IDT and the QPC, an unwanted potential fluctuation at a QPC arises, hence reducing the accuracy of the quantized current value of the plateau. In this work, we have studied the effect of unwanted rf-coupling to the current plateau.

II. EXPERIMENTS AND DISCUSSION

The Figure 1 is a schematic diagram of the device. A metallic split gate was used to serve as a QPC to form a quasi one-dimensional conduction channel while an IDT was used to produce SAW. SEM picture of the fabricated QPC is shown in the figure. The width of the QPC gate is around $2\ \mu\text{m}$, and the gap between the two metallic gates is around $800\ \text{nm}$. To generate $1\ \mu\text{m}$ -long SAW, we kept the spacing between the IDT gates at $500\ \text{nm}$. To achieve the maximum efficiency for an IDT, we kept the width and the length of the gates at $250\ \text{nm}$, and $100\ \mu\text{m}$, respectively. The overlap between the upper and the lower electrodes of an IDT is $70\ \mu\text{m}$, and 70 pairs of gates are used. To minimize the stray capacitance between the IDT and the QPC, we placed the IDT $3\ \text{mm}$ away from the QPC region. The devices were fabricated on the surface of an $80\ \text{nm}$ -deep 2-dimensional electron gas (2DEG) layer based on a GaAs/AlGaAs heterostructure with an electron density of $2.2 \times 10^{11}\ \text{cm}^{-2}$ and a mobility of $3 \times 10^6\ \text{cm}^2\text{V}^{-1}\text{s}^{-1}$ at $4.2\ \text{K}$. First, the mesa was defined by chemical etching in a $\text{H}_2\text{O}_2 : \text{H}_3\text{PO}_4 : \text{H}_2\text{O}$ (1:1:50) solution, which gives an etch rate of around $100\ \text{nm}/\text{min}$ at room temperature. To form Ohmic contacts, $30\ \text{\AA}$ of

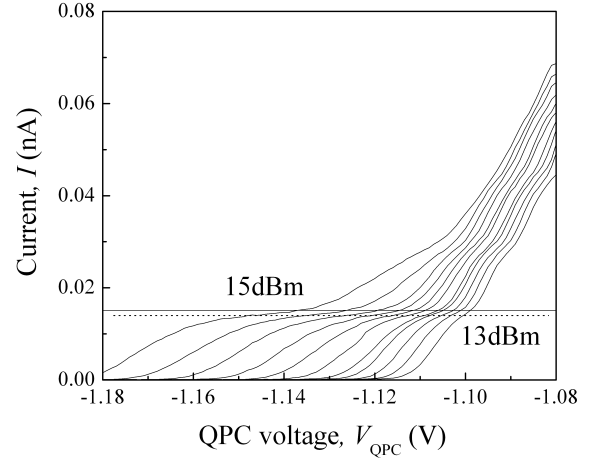


Fig. 2. The acousto-electric currents as a function the QPC gate voltages at various SAW powers. The frequency of the applied SAW was $2.82794\ \text{GHz}$, and the power of the rf signal applied to an IDT was changed from $13\ \text{dBm}$ to $15\ \text{dBm}$ in 0.2-dBm steps. The horizontal dashed line is a guide line indicating a current value of $0.0139\ \text{nA}$.

Ni, $2000\ \text{\AA}$ of Au, and $1000\ \text{\AA}$ of Ge, followed by $750\ \text{\AA}$ of Ni, were evaporated and annealed at 420°C in Ar gas atmosphere for 60 seconds. The QPCs were fabricated by using electron beam lithography. A single layer of $950\text{k}\ 5\%$ PMMA in anisole was used for an e-beam resist. After the e-beam writing and the development, thermal evaporation of $150\ \text{\AA}$ of Ti, followed by $150\ \text{\AA}$ of Au was done to form a QPC gate. After the fabrication of a QPC, an IDT was fabricated with the same e-beam lithography process, and $70\ \text{\AA}$ of Ti and $150\ \text{\AA}$ of Au were used for IDT gates. Finally, large electrical contact pads were fabricated with optical lithography.

The measurements were done at around $T = 1.2\ \text{K}$. The samples were cooled down with a positive voltage (typically $+0.3\ \text{V}$) on the gate to minimize the random telegraph noise of the QPC. Semi-rigid coaxial cables were installed on the insert to deliver rf signals for the IDT. The sample carrier was designed to minimize the rf-coupling between the rf signal line and the DC measurement lines including the gate electrodes. Applying the high power rf signal to IDT has been found to cause considerable heat dissipation on the sample area, resulting in the elevation of the electron temperature of the sample. Also, a random telegraph noise (RTN) was observed in the acousto-electric current when high-power of rf signals were applied to the IDT continuously. To avoid such a temperature change and RTN at high SAW powers, rf signals were applied in a pulse mode with a duty cycle of $D = 1/30$ rather than applying a continuous rf signal. This makes the acousto-electric current $I < nef \times D$, because rf signal delivered by the pulse mode is usually lower than the duty cycle ratio. Here, the duty cycle D is defined by τ/T , where τ is the pulse duration time per cycle and T is the period of a pulse.

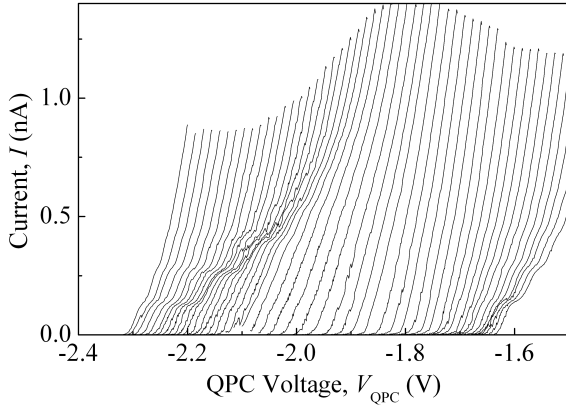


Fig. 3. The acousto-electric currents as a function of the QPC gate voltage at different SAW frequencies. The applied SAW power was kept at 13 dBm while the frequencies were varied from 2.8271 GHz to 2.8276 GHz in 10 kHz steps. For clarity, each curve was shifted by -15 mV in gate voltage as the SAW frequency was increased by 10 kHz.

Figure 2 shows the acousto-electric current measured at various SAW powers. A few plateaus were found around $I = efD, 2efD, 3efD$, and so on. The first plateau was formed around 0.0139 nA which is slightly smaller than $I = ef \times D (0.0151 \text{ nA})$ shown as a solid horizontal line in the figure. The plateau currents stay at the same currents even though the SAW power is increased. However, the positions of the plateaus in QPC gate voltage were shifted to lower QPC gate voltages as the SAW power were increased. This is a typical signature of SAW-induced acousto-current plateau behavior [11].

Figure 3 shows the frequency dependance of the current plateaus. The acousto-electric currents were measured by varying the SAW frequencies from 2.8271 GHz to 2.8276 GHz in 10 kHz steps while the SAW power was fixed to 13 dBm. As it can be seen from the figure, the signals on the right and the left sides of the figure show clear current plateau, while no plateaus are seen in the middle of the graph. When rf-signals are applied to the IDT, the most of the applied rf-signals are reflected from the IDT due to the impedance mismatch between the transmission line and the IDT. Since there is a stray capacitance between the rf transmission line and the QPC gates even though they are 3 mm apart, some of the reflected rf-signals can be picked up by the QPC gates. Hence, this rf-coupling induces unwanted potential fluctuations on QPC gates. Such coupling of unwanted rf-signals to the gate can cause a nonadiabatic charge transfer process to hinder the formation of current plateaus.

Figure 4 shows the acousto-electric current as a function of SAW frequency. The SAW frequencies were varied from 2.81 GHz to 2.84 GHz while the SAW power and the gate voltage were set to 13 dBm and -2.17 V, respectively. As it can be seen from the figure, the acousto-electric currents show a resonance peak with a center

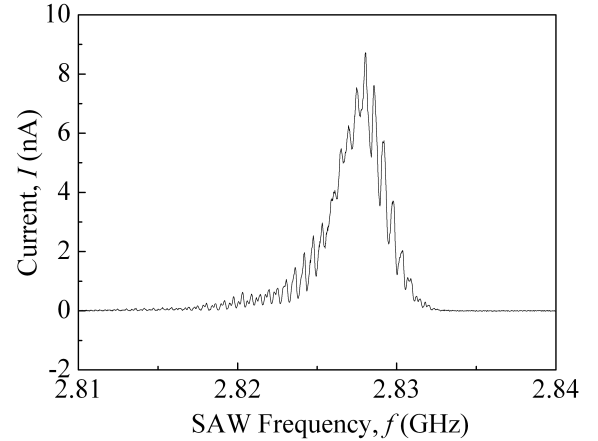


Fig. 4. The acousto-electric current as a function of the applied SAW frequency. The QPC gate voltage was set to -2.17 V, and the SAW power was set to 13 dBm.

frequency of 2.828 GHz. In addition to the resonance peak, small periodic fluctuations of the acousto-electric currents were observed. If the rf signals were turned off before the SAW reaches the QPC by reducing the duty cycle, no interference in acousto-electric current was observed. Also, when the IDT was placed closer to the QPC, the amplitude of periodic fluctuations in the currents became larger. These are clear indications of the interference between the SAW-induced signals and the rf pick-up signals on the QPC gate. The SAW travels at a velocity of 2800 m/s [14] while the electro-magnetic field travels at the speed of light. Thus the phase of the rf pick-up signals on the QPC is almost identical to the applied rf signals because the pick-up is immediate, while the phase of the SAW on the QPC depends on the frequency of the SAW. Because the SAW velocity is a constant at any SAW frequencies, the SAW velocity v can be defined by $v = f\lambda$, where λ is a SAW wave length. Thus, the phase of the SAW at the entrance of the QPC gate becomes $\phi = 2\pi l/\lambda$, where l is the distance between the QPC gate and the IDT. Hence, the superposition of these signals causes interference that depends on the SAW frequency. The amplitude of this interference depends on the stray capacitance between the IDT gates and the QPC gates.

Figure 5 shows the correlation between the interference and the formation of the current plateau. The transconductance of the acousto-electric current was derived by numerically differentiating the acousto-electric current (from Fig. 3) with respect to the gate voltage. Figure 5(a) shows a pseudo color plot of the transconductance as a function of SAW frequency and the gate voltage. The formation and the destruction of the current plateaus are clearly seen from the figure as the SAW frequency varies. Figure 5(b) is the acousto-electric current as a function of frequency at a fixed QPC gate voltage. The frequency range covers almost one cycle of the interferences in the acousto-electric currents. The expected

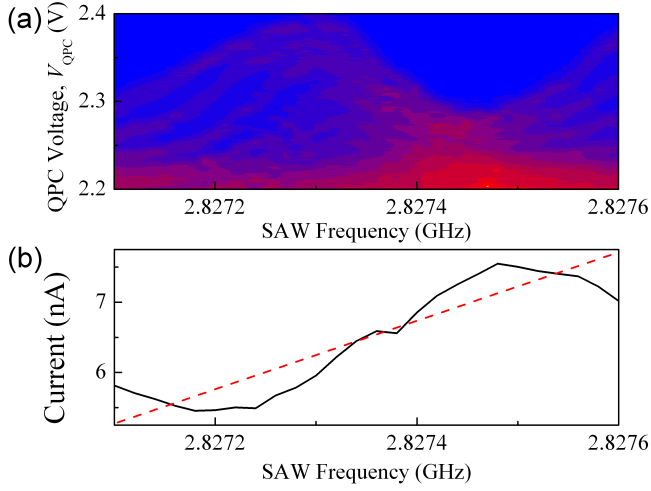


Fig. 5. (a) Pseudo-color plot of the transconductance (dI/dV_g) taken at various SAW frequencies and the QPC gate voltages. Blue color corresponds to zero transconductance while red color corresponds to higher transconductance than zero. (b) The acousto-electric current from 2.8271 GHz to 2.8276 GHz when the QPC gate voltage was set to -2.17 V and the SAW power was set to 13 dBm. The red dashed line is a guide line presumed for a signal with no interference.

currents with no interference are marked as a red dashed line in the figure, to distinguish the frequency regions for ‘constructive’ and ‘destructive’ interferences. Here, the words ‘constructive’ and ‘destructive’ were used in the sense that the constructive or the destructive interference resulted in increased or decreased current compared to the current without rf coupling. By comparing the two figures, it is clear that the formation of the current plateau arises only when the interference between the pick-up signal and the SAW signal is destructive. Also, it is clear that the current plateau totally vanishes for the constructive interference region. As it can be seen from Fig. 3, the overall current is larger in the middle of the graph where no plateau is observed. From this, we suspect that somehow quantum dots are carrying more electrons than necessary in the constructive interference region to destroy the current plateaus.

III. CONCLUSIONS

Electron charge pumps are fabricated by exploiting acousto-electric currents through a QPC induced by SAW. The observed acousto-electric currents showed a few current plateaus as a function of the QPC gate voltages. However, there is a strong correlation between the formation of current plateaus and the applied SAW frequencies. We found that the constructive coupling between the rf signal and the SAW is responsible for the destruction of the current plateaus. Our experimental results show that careful shielding of rf signals is nec-

essary to achieve accurate plateaus for current-standard applications.

ACKNOWLEDGMENTS

The authors are grateful to Dr. Chris Ford for fruitful discussions. This work was supported by the Korea Research Institute of Standard and Science. YC was supported for two years by a Pusan National University Research Grant.

REFERENCES

- [1] U. Meirav, M. A. Kastner and S. J. Wind, *Phys. Rev. Lett.* **65**, 771 (1990).
- [2] M. Field, C. G. Smith, M. Pepper, D. A. Ritchie, J. E. F. Frost, G. A. C. Jones and D. G. Hasko, *Phys. Rev. Lett.* **70**, 1311 (1993).
- [3] A. T. Johnson, L. P. Kouwenhoven, W. de Jong, N. C. van der Vaart and C. J. P. M. Harmans, *Phys. Rev. Lett.* **69**, 1592 (1992).
- [4] L. P. Kouwenhoven, A. T. Johnson, N. C. van der Vaart and C. J. P. M. Harmans, *Phys. Rev. Lett.* **67**, 1626 (1991).
- [5] L. J. Geerligs, V. F. Anderegg, P. A. M. Holweg, J. E. Mooij, H. Pothier, D. Esteve, C. Urbina and M. H. Devoret, *Phys. Rev. Lett.* **64**, 2691 (1990).
- [6] M. D. Blumenthal, B. Kaestner, L. Li, S. Giblin, T. J. B. M. Janssen, M. Pepper, D. Anderson, G. Jones and D. A. Ritchie, *Nature Physics* **3**, 343 (2007).
- [7] B. Kaestner, V. Kashcheyevs, S. Amakawa, M. D. Blumenthal, L. Li, T. J. B. M. Janssen, G. Hein, K. Pierz, T. Weimann, U. Siegner and H. W. Schumacher, *Phys. Rev. B* **77**, 153301 (2008).
- [8] B. Kaestner, V. Kashcheyevs, G. Hein, K. Pierz, U. Siegner and H. W. Schumacher, *Appl. Phys. Lett.* **92**, 192106 (2008).
- [9] V. I. Talyanskii, J. M. Shilton, M. Pepper, C. G. Smith, C. J. B. Ford, E. H. Linfield, D. A. Ritchie and G. A. C. Jones, *Phys. Rev. B* **56**, 15180 (1997).
- [10] J. Cunningham, V. I. Talyanskii, J. M. Shilton, M. Pepper, M. Y. Simmons and D. A. Ritchie, *Phys. Rev. B* **60**, 4850 (1999).
- [11] J. Cunningham, V. I. Talyanskii, J. M. Shilton, M. Pepper, A. Kristensen and P. E. Lindelof, *Phys. Rev. B* **62**, 1564 (2000).
- [12] P. J. Leek, M. R. Buitelaar, V. I. Talyanskii, C. G. Smith, D. Anderson, G. A. C. Jones, J. Wei and D. H. Cobden, *Phys. Rev. Lett.* **95**, 256802 (2005).
- [13] Yun-Sok Shin, Yun-Sok Shin, Woon Song, Jinhee Kim, Byung-Chill Woo, Nam Kim, Myung-Hwa Jung, Soo-Hyeon Park, Jong-Gi Kim, Kang-Hun Ahn and Kimin Hong, *Phys. Rev. B* **74**, 195415 (2006).
- [14] J. Ebbecke, N. E. Fletcher, T. J. B. M. Janssen, F. J. Ahlers, M. Pepper, H. E. Beere and D. A. Ritchie, *Appl. Phys. Lett.* **84**, 4319 (2004).